Biochimica et Biophysica Acta 1858 (2016) 386–392

Contents lists available at ScienceDirect

Biochimica et Biophysica Acta

journal homepage: www.elsevier.com/locate/bbamem

Single molecule experiments emphasize GM1 as a key player of the different cytotoxicity of structurally distinct Aβ1–42 oligomers

Martino Calamai [a,b,*], Elisa Evangelisti [c], Roberta Cascella [c], Niccoló Parenti [a], Cristina Cecchi [c,d], Massimo Stefani [c,d], Francesco Pavone [a]

[a] European Laboratory for Non-linear Spectroscopy (LENS), University of Florence, 50019 Florence, Italy
[b] National Institute of Optics, National Research Council of Italy (CNR), Largo Fermi 6, 50125, Florence, Italy
[c] Dipartimento di Scienze Biomediche Sperimentali e Cliniche "Mario Serio", Università degli Studi di Firenze, 50134 Florence, Italy
[d] Centro Interuniversitario per lo Studio delle Malattie Neurodegenerative (CIMN), 50134 Florence, Italy

ARTICLE INFO

Article history:
Received 1 July 2015
Received in revised form 10 November 2015
Accepted 3 December 2015
Available online 4 December 2015

Keywords:
GM1 ganglioside
Single molecule tracking
Aβ oligomers
Alzheimer's disease

ABSTRACT

It is well established that cytotoxic Aβ oligomers are the key factor that triggers the initial tissue and cell modifications eventually culminating in the development of Alzheimer's disease. Aβ1–42 oligomers display a high degree of polymorphism, and several structurally different oligomers have been described. Amongst them, two types, recently classified as A+ and A−, have been shown to possess similar size but distinct toxic properties, as a consequence of their biophysical and structural differences. Here, we have investigated by means of single molecule tracking the oligomer mobility on the plasma membrane of living neuroblastoma cells and the interaction with the ganglioside GM1, a component of membrane rafts. We have found that A+ and A− oligomers display a similar lateral diffusion on the plasma membrane of living cells. However, only the toxic A+ oligomers appear to interact and alter the mobility of GM1. We have also studied the lateral diffusion of each kind of oligomers in cells depleted or enriched in GM1. We found that the content of GM1 influences the diffusion of both types of oligomer, although the effect of the increased levels of GM1 is higher for the A+ type. Interestingly, the content of GM1 also affects significantly the mobility of GM1 molecules themselves.

1. Introduction

A plethora of recent results supports the hypothesis that Aβ oligomers are the cytotoxic species mainly responsible for the initial biochemical and functional alterations eventually culminating with the development of Alzheimer's disease [1]. Accordingly, several therapeutic strategies are now directed at finding antibodies to specifically reduce the appearance of Aβ oligomers [2,3]. However, the structure of Aβ oligomers is not unique, and oligomers with different conformations and cytotoxic properties have been described in the past [4–7]. These alternative structures can be obtained *in vitro* using different conditions of aggregation. Recently published results show that Aβ1–42 oligomers of comparable size but different structure and biophysical properties can display different toxicities [8]. In this case, the oligomers were classified as A+ or A−, according to their ability to be recognized by the conformation-specific antibody A11 [9]. A+ oligomers were found to be more toxic than A− oligomers, possibly as a consequence of the increased exposure of hydrophobic residues that would destabilize them and favour their interaction with the plasma membrane.

In general, Aβ1–42 oligomer binding to the plasma membrane appears to be the preliminary trigger for several downstream mechanisms of toxicity [10,11]. The ganglioside GM1, a component of membrane rafts involved in neurodevelopment and neuroprotection, has been found to interact with specific types of Aβ1–42 oligomers [11–14], commonly referred to as ADDLs (amyloid β-derived diffusible ligands) [15]. Moreover, even a modest depletion of GM1 content can decrease the degree of interaction of Aβ1–42 oligomers with the plasma membrane [11]. We have recently shown that distinct Aβ1–42 oligomers recognized by the conformation specific antibody OC and I11, respectively, diffuse differently on the plasma membrane of living cells [16] and that Aβ1–42 oligomers alter the mobility of single GM1 molecules upon binding [12]. Here, we further investigated the GM1/Aβ1–42 relation by studying the mobility of A+ and A− oligomers on the plasma membrane of neuronal SH-SY5Y cells by Single Molecule Tracking (SMT) experiments.

2. Materials and methods

2.1. Preparation and characterization of Aβ1–42 oligomers

Aβ1–42 oligomers were prepared as described previously [8]. In brief, the lyophilised peptide was dissolved in 100% hexafluoro-2-

* Corresponding author at: European Laboratory for Non-linear Spectroscopy (LENS), University of Florence, 50019 Florence, Italy.
E-mail address: calamai@lens.unifi.it (M. Calamai).

http://dx.doi.org/10.1016/j.bbamem.2015.12.009
0005-2736/

isopropanol (HFIP) to 1.0 mM and then the solvent was evaporated. Aβ1–42 oligomers were prepared by suspending the peptide at the same concentration in 50 mM NaOH and diluting this solution in PBS to a final Aβ1–42 concentration of 25 μM. Then, the sample was centrifuged at 22,000 r.c.f. for 30 min, the pellet discarded and the supernatant incubated at 25 °C without agitation for 1 day to obtain A+ oligomers or for 4 days to obtain A− oligomers [8]. Aβ1–42 fibrils were obtained at a final concentration of 50 μM after 4 days of incubation. Dot-blot analysis of Aβ1–42 oligomers was performed by spotting 2.0 μl (25 μM) of each conformer onto a polyvinylidene fluoride (PVDF) membrane. After overnight blocking (1.0% bovine serum albumin in TBS/TWEEN 0.1%) the blots were probed with A11 (Life Technologies), OC (Millipore), or 6E10 (Signet) antibodies and then incubated with the appropriate horseradish peroxidase-conjugated secondary antibodies. The immunolabelled bands were detected using a SuperSignal West Dura (Pierce, Rockford, IL, USA).

2.2. Cell cultures

Human SH-SY5Y neuroblastoma cells (A.T.C.C. Manassas, VA, USA) were cultured in Dulbecco's Modified Eagle's Medium (DMEM), F-12 Ham with 25 mM HEPES and $NaHCO_3$ (1:1) supplemented with 10% FBS, 1.0 mM glutamine and 1.0% penicillin and streptomycin solution. Cell cultures were maintained in a 5.0% CO_2 humidified atmosphere at 37 °C and grown until 80% confluence for a maximum of 20 passages.

2.3. Single molecule imaging and tracking

Quantum dot (QD) labelling and live imaging of oligomers and GM1 have been extensively described [12–16]. Briefly, living cells previously exposed to 10 μM monomer equivalent of Aβ1–42 A+ and A− oligomers were incubated in phenol red-free Leibovitz's L-15 medium 10% FBS at 37 °C with anti-Aβ 6E10 (Signet, Dedham, MA) primary antibody (1:1000) for 20 min. Biotinylated anti-mouse (Jackson Laboratories) Fab antibodies were used as secondary antibodies at 1:400 dilution for 5 min. Streptavidin-coated QDs (Invitrogen) emitting at 655 nm were used at 1:10,000 dilution for 1.0 min. For single molecule GM1 experiments, the cells were incubated first with anti-Aβ 6E10 antibody (1:1000) for 20 min, then for 5 min with anti-mouse Alexa Fluor 488 (Invitrogen, 1:500) and 10 μg/ml biotinylated CTXB, and finally with streptavidin QDs 655 (1:10,000) in QD binding buffer for 1.0 min. The cells were monitored with a custom-made wide-field epifluorescence microscope equipped with an oil-immersion objective (Nikon Plan Apo TIRF 60x/1.45), a Reliant 150 Select argon ion laser (excitation line 488 nm) and a heating chamber. The emission filters (Semrock) were FF499-Di01-25 dichroic, FF01-655/15-25 (for QDs) and FF01-530/43-25 (for Alexa 488). Movies were acquired with an integration time of 30 or 100 ms with an Electron Multiplying Charge-Coupled iXon camera (Andor). Recording sessions did not last more than 30 min.

Tracking of single QDs, identified by their fluorescence intermittence, was performed with MATLAB (MathWorks, Natick, MA) using a homemade macro that accounts for blinking in the fluorescence signal [17–19]. In brief, the method consisted of two main steps, applied successively to each frame of the sequence. First, the fluorescent spots were detected by cross-correlating the image with a Gaussian model of the Point Spread Function. A least-squares Gaussian fit was applied (around the local maximum above a threshold) to determine the centre of each spot with a spatial accuracy of 10–20 nm (depending on the signal-to-noise ratio). Second, QD trajectories were assembled automatically by linking, frame to frame, the centres of the fluorescent spots likely coming from the same QD. The association criterion was based on the assumption of free Brownian diffusion and took into account short blinking events. After completion of the process, a manual association step was performed, in which QD trajectories of maximal length were assembled from smaller fragments separated by longer blinking events that were not taken into account by the automatic linking procedure. For single molecule tracking experiments, we incubated the cells with CTXB for times shorter than for standard immunolabelling experiments, thus obtaining a lower level of labelling. The concentration of streptavidin-QDs was largely in excess with respect to biotin-CTXB. Therefore, most, if not all, of the CTXB molecules bound to the plasma membrane are expected to be labelled.

2.4. Quantitative analysis of the diffusion coefficient

The mean square displacement (MSD) analysis allows for calculating the initial diffusion coefficient (D) of each particle [18,19]. Briefly, physical parameters can be extracted from each trajectory (x(t),y(t)) by computing the MSD [20], as calculated from the following formula:

$$\mathrm{MSD}(ndt) = \frac{1}{N-n}\sum_{i=1}^{N-n}\left[(\mathrm{X}_{(i+n)}-\mathrm{X}_i)^2 + \left(\mathrm{y}_{(i+n)}-\mathrm{y}_i\right)^2\right]$$

where x_i and y_i are the coordinates of a particle on frame i, dt is the time between two successive frames, N the total number of frames of the trajectory and ndt the time interval over which the displacement is averaged. This function enables the analysis of the lateral dynamics on short (initial diffusion coefficient) and long (types of motion) time scales. Different types of motion can be distinguished from the time dependence of the MSD [20]. The initial diffusion coefficient (D) is determined by fitting the initial 2 to 5 points of the MSD against time plot with $\mathrm{MSD(t)} = 4\mathrm{D}_{2\text{-}5}\,\mathrm{t} + \mathrm{b}$.

2.5. Modulation and evaluation of membrane GM1 content

SH-SY5Y cells were seeded on glass coverslips and treated with 25 μM D-threo-1-phenyl-2-decanoylamino-3-morpholino-1-propanol (PDMP; Matreya LLC, Pleasant Gap, PA, USA), an inhibitor of GM1 synthesis, or with 100 μg/ml bovine brain GM1 (Sigma-Aldrich) and incubated for 48 h at 37 °C. Cytotoxicity of PDMP was assessed by the MTT assay as previously reported [21]. After incubation for 48 h at 37 °C, the cells were loaded with 2.25 μg/ml CTXB and analysed using a FACS Canto flow cytometer (Beckton Dickinson Biosciences, San Jose, CA, USA). The measured fluorescence intensities were expressed as fractional changes above the resting baseline, $\Delta F/F$, where F is the average baseline fluorescence in control cells with basal GM1 content (taken as 100%) and ΔF represents the fluorescence changes over the baseline in PDMP- or GM1-treated cells [13]. The SH-SY5Y cells were also seeded on glass coverslips and treated with 4.5 μg/ml Alexa Fluor 647-conjugated CTXB or, alternatively, with 1:100 diluted rabbit polyclonal anti-GM1 antibodies (Calbiochem, EMD Chemicals Inc., Darmstadt, Germany) and then with Alexa Fluor 488-conjugated anti-rabbit secondary antibodies diluted 1:1000. The emitted fluorescence was detected after excitation at 647 and 488 nm, respectively, using a confocal Leica TCS SP5 scanning microscope (Mannheim, Germany) equipped with an argon laser source. A series of 1.0 μm thick optical sections (1024 × 1024 pixels) was taken through the cell depth for each sample using a Leica Plan Apo 63× oil immersion objective and projected as a single composite image by superimposition.

2.6. Statistical analysis

D values are log normally distributed. Statistical significance was evaluated by ANOVA test performed on the log normal distributions. A p value < 0.05 was considered statistically significant. The data analysed were obtained from three independent experiments.

3. Results

3.1. A + and A − oligomer dynamics on the cell membrane

We have investigated the membrane dynamics of A + and A − Aβ1–42 oligomers, which have similar size but display different cytotoxicity [8]. The conformational properties of Aβ1–42 monomer, oligomers and fibrils were evaluated by immunoblot analysis using antibodies specific for prefibrillar (A11) and fibrillar (OC) oligomers (Fig. 1a) according to Ladiwala et al. [8]. The proper loading of each Aβ1–42 assembly was confirmed by the sequence-specific antibody 6E10, which recognizes the N terminus of Aβ1–42 (Fig. 1a). The preformed oligomers were incubated with SH-SY5Y human neuroblastoma cells for 20 min and labelled with primary 6E10 antibodies and secondary antibodies coupled to quantum dots (QDs) emitting at 655 nm (Fig. 1b). Although incubated with the cells at the same concentration, the average number of single-QD-labelled A + oligomers per cell was two folds higher than A −. In order to be confident on the nature of the species observed, we incubated the cells with monomers and fibrils in place of A + and A − oligomers. We found that monomers and fibrils do not bind significantly to the cells under the conditions examined here (see Supplementary Movies 1 and 2). These results suggest that if any dissociation or fibrillation of oligomers occurs during the incubation time, it is unlikely to be detected as these species do not bind to the cells (or the epitope may not be accessible to the antibody in case of the monomer). We conclude that what we image in our recordings are the oligomeric species. The majority of individual oligomers of both types appeared confined, with few following Brownian motion (Fig. 1c,d and Supplementary Movie 3). Interestingly, A + and A − oligomers displayed a median lateral diffusion coefficient comparable to that of Aβ1–42 ADDL oligomers labelled with the conformational antibody I11, specific for non-fibrillar species and analogue to the A11 antibody that recognizes A + oligomers [9] (Table 1). However, the mobility of the different types of Aβ oligomers was higher than that observed for other amyloid aggregates [16]. The faster diffusion was not attributable simply to the smaller size of these oligomers, as their measured sizes were comparable (approximately 4–6 nm [8]). In addition, the use of synthetic giant unilamellar vesicles (GUVs) led us to propose that the

Table 1
Diffusion coefficients[a] of different Aβ1-42 oligomers on the plasma membrane of SH-SY5Y neuroblastoma cells[b].

Oligomers (primary antibody)	GM1 depleted D_{median} ($\mu m^2\ s^{-1}$)	GM1 Basal D_{median} ($\mu m^2\ s^{-1}$)	GM1 enriched D_{median} ($\mu m^2\ s^{-1}$)
Aβ1–42 A + (6E10)	1.2×10^{-2}	8.7×10^{-3}	3.8×10^{-4}
Aβ1–42 A − (6E10)	3.3×10^{-2}	5.9×10^{-3}	3.7×10^{-3}
Aβ1–42 ADDLs (DE2B4)[c]		6.1×10^{-4}	
Aβ1–42 ADDLs (OC)[c]		9.4×10^{-4}	
Aβ1–42 ADDLs (I11)[c]		4.0×10^{-3}	
GM1[d]	1.7×10^{-1}	6.7×10^{-2}	1.8×10^{-2}

[a] Since the diffusion coefficients are distributed over several orders of magnitude, we report the median value instead of the mean value.
[b] Cells were incubated with distinct oligomers solutions.
[c] Data from [15].
[d] GM1 labelled with biotin-CTXB associated to streptavidin-655QDs.

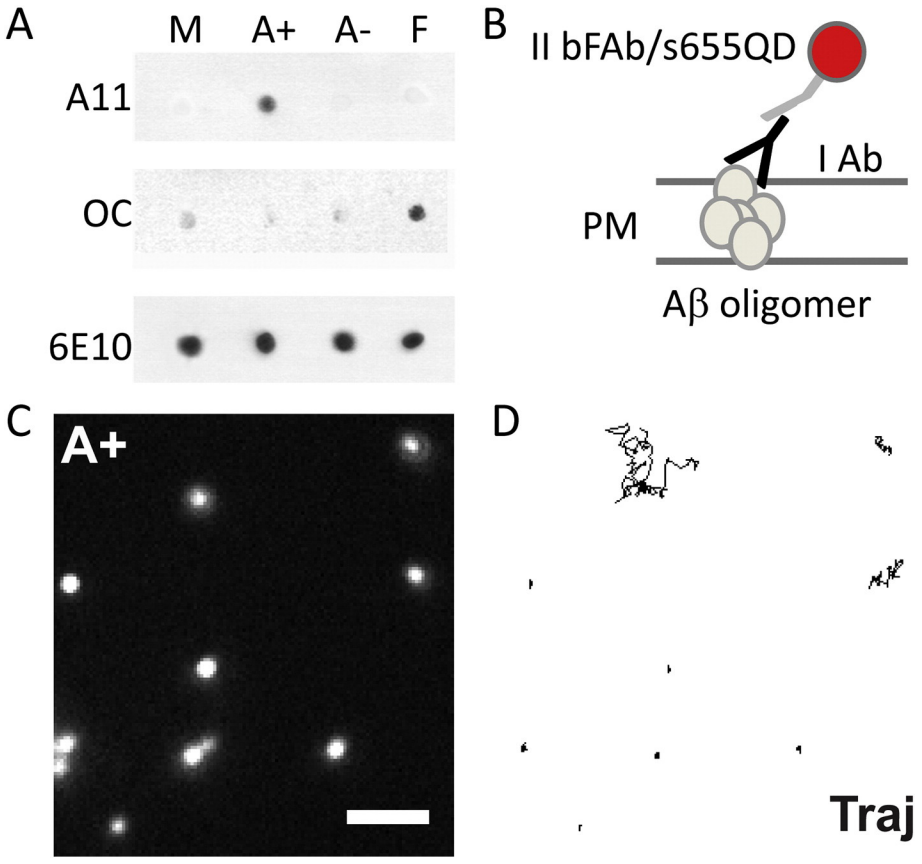

Fig. 1. Dot-blot analysis and SMT of A + and A − Aβ1–42 oligomers. A) Conformation-specific antibody analysis of Aβ assembly. The Aβ1–42 monomer (M) and the A + and A − oligomers (25 μM monomer equivalents) and fibrils (F) (50 μM monomer equivalents) were assembled for 1–4 days (without agitation), and then deposited on PVDF membranes. Afterward, the membranes were probed with conformation-specific (A11, prefibrillar oligomers (top), OC, fibrillar conformers (middle) and sequence-specific (6E10, N-terminus of Aβ (bottom)) antibodies. B) General surface labelling scheme of Aβ oligomers on the plasma membrane (PM). The cells were incubated with distinct oligomers solutions and labelled with primary (Ab) and secondary biotinylated Fab antibodies coupled to streptavidin 655QDs (bFAb/s655QD). B) and C) Example of single A + oligomers on the plasma membrane of living SH-SY5Y cells and corresponding trajectories extrapolated from the recordings. Scale bar 2 μm.

slow diffusion of Aβ1–42 oligomers can be in general attributable to their interaction with cellular structures [16]. Although the subtle differences in structure between A+ and A− oligomers do not appear to influence significantly their mobility, they can affect the amount of oligomers bound to the plasma membrane which, in turn, appears to be related to the degree of cytotoxicity.

3.2. Influence of A + oligomers on GM1 membrane dynamics

In the light of recent results showing the impact of amyloid oligomers on GM1 dynamics [12–22], we have sought to define conditions in which A+ and A− oligomers affected the mobility of GM1. Similar to previous experiments, we labelled the oligomers bound to the plasma membrane with primary and secondary Alexa488 antibodies (Fig. 2a), whereas GM1 was labelled with biotinylated-cholera toxin subunit B (CTXB) and streptavidin-655QDs. Interestingly, we found some GM1 molecules co-localizing with A+ aggregates (Fig. 2b, Supplementary Movie 4). The mean square displacement (MSD) against time plot revealed that these GM1 molecules displayed a limited type of motion, instead of the Brownian motion observed in general (Fig. 2c). On the other hand, in the case of A− oligomers, we could not find any overlap with GM1 molecules. These results show clearly that the toxic A+ oligomers interact with GM1. These data further confirm the direct implication of GM1, a constituent of membrane rafts, in the pathogenic cascade triggered by amyloid oligomers.

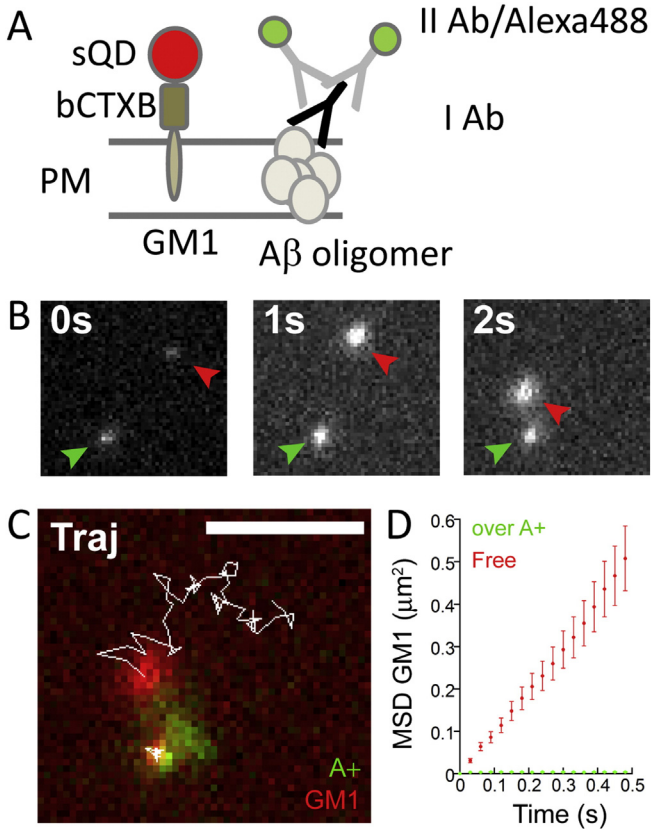

Fig. 2. SMT of GM1 in the presence of A+ oligomers. A) General surface labelling scheme of GM1 and Aβ oligomers on the plasma membrane. The cells were incubated with solutions of either oligomer type, which was labelled with primary and secondary Alexa488 antibodies. GM1 was labelled with biotinylated CTXB (bCTXB) coupled to streptavidin 655QDs. B) Example of freely moving (red) or confined (green) single GM1 molecules on the plasma membrane of living SH-SY5Y cells. C) Trajectories extrapolated from the recordings in B superimposed to the image of GM1 (red) and A+ oligomers (green). Scale bar 2.0 μm. D) Plot of MSD against time showing that the different dynamic behaviour of the two GM1 molecules in B and in C is dependent on the co-localization with A+ oligomers.

3.3. Influence of GM1 on A + membrane dynamics

As membrane GM1 binds differently to either type of oligomers and the latter influence differently GM1 mobility on the cell membrane, we tested whether and how changes in the GM1 content affected oligomer mobility. In order to decrease or to increase the amount of GM1 in the plasma membrane, SH-SY5Y cells were treated with 25 μM D-threo-1-phenyl-2-decanoylamino-3-morpholino-1-propanol (PDMP), an inhibitor of GM1 synthesis, or with 100 μg/ml bovine brain GM1, respectively. Confocal images of cells labelled either with anti-GM1 antibody and secondary Alexa488 antibody, or CTXB-Alexa647, showed depletion or enrichment in GM1 after either treatment (Fig. 3a). Quantitative FACS flow cytometer analysis of CTXB-Alexa647 labelled cells confirmed significant changes with respect to the untreated control cells with basal GM1 content (Fig. 3b). A dose-dependent curve of cell viability showed the absence of any PDMP cytotoxicity at our experimental conditions (Fig. 3c).

Initially, we used the so-treated cells to investigate, by SMT, the effect of altered GM1 content on GM1 dynamics in the membrane, a study never reported before. The average MSD was calculated from the trajectories of single GM1 molecules labelled with biotin-CTXB associated with streptavidin-655QDs (Fig. 4a, b and Supplementary Movie 5). The linear fitting of the data displayed in the plot of MSD against time suggested that GM1 molecules display Brownian diffusion under all the conditions analysed here (Fig. 4c). However, the distribution of the initial diffusion coefficients (D) extrapolated from the MSD of each GM1 molecule highlighted significant changes (Fig. 4d). The overlapping of the distributions under different conditions is a general consequence of SMT experiments, whose strength is to show how spread the measured values are. The diffusion coefficients of a biological molecule obtained by SMT can be distributed over several orders of magnitude [19]. With respect to cells at basal conditions, the median D value

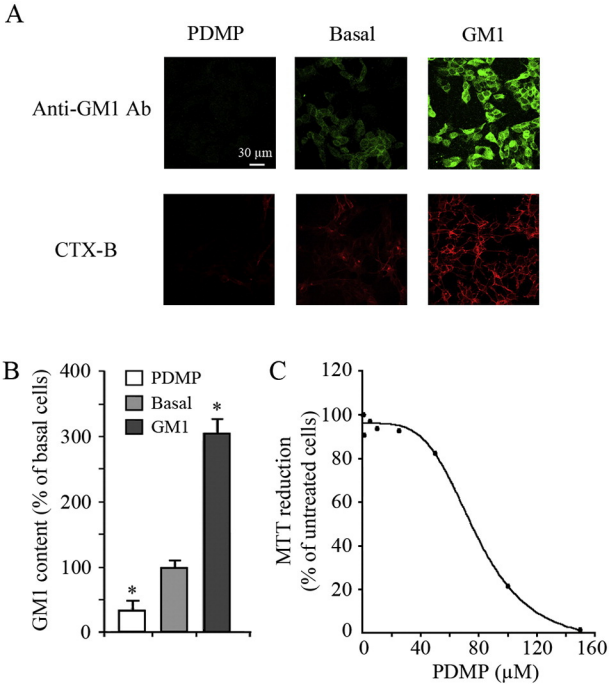

Fig. 3. Alterations of GM1 content. A) Confocal images of cells incubated with 25 μM PDMP (depleted), or with 100 μg/ml bovine brain GM1 (enriched) for 48 h, or cell culture medium and labelled with anti-GM1 antibody and secondary Alexa488-antibody (green), or CTXB-Alexa647 (red). B) FACS flow cytometer analysis of CTXB-Alexa647 labelled cells treated as above. The values are means ± s.d. of three independent experiments, (*) indicates significant differences relative to untreated control cells (basal) ($p \leq 0.05$). C) Dose-dependence curve of PDMP cytotoxicity assessed by the MTT assay. Cell viability was expressed as percent of MTT reduction in treated cells with respect to untreated cells (taken as 100%).

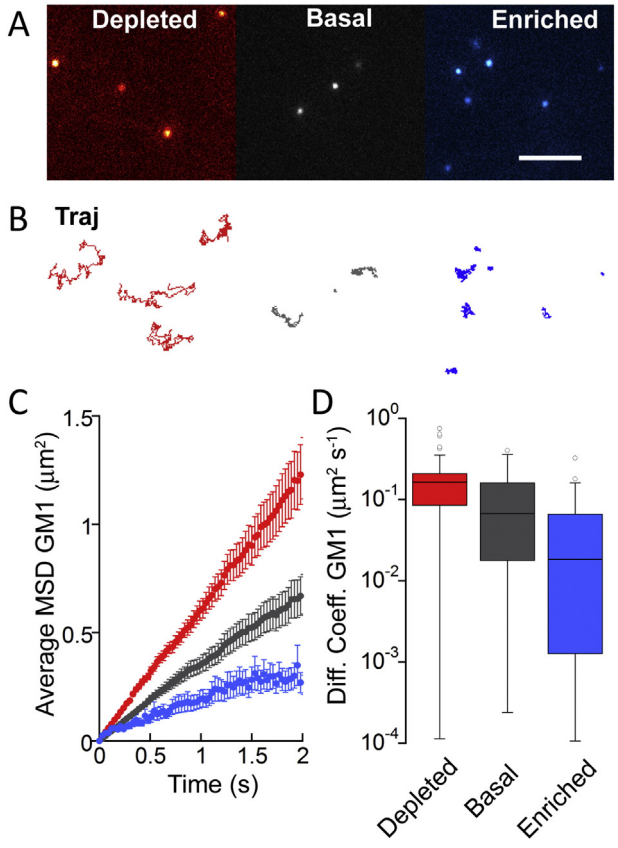

Fig. 4. The content of GM1 influences its own lateral diffusion. A) SMT of GM1 labelled with bCTXB coupled to s655QD in cells in basal conditions (grey), or treated with 25 μM PDMP (red) and 100 μg/ml bovine brain GM1 (blue). Scale bar 5.0 μm. B) Trajectories extrapolated from the recordings in A. C) Average mean square displacement of GM1 molecules (n > 90 for each condition). D) Box plot of diffusion coefficients of single GM1 molecules in cells with basal or modified GM1 content. ANOVA analysis of log normal distributed data, F statistic = 33.9, $p < 0.0001$.

increased by two folds or decreased by three folds in cells depleted and enriched in GM1, respectively (Table 1). These changes in membrane fluidity in relation to the content of GM1 could affect the interaction and localization of membrane proteins, and might be of relevance also when considering the role of GM1 in neurodevelopment and neuroprotection [23].

Then, the cells depleted or enriched in GM1 were incubated with A+ or A− oligomers labelled with 6E10 antibody and 655QDs, as described above. ANOVA analysis of the log-normally distributed D values indicated that the GM1 content significantly affected the dynamic behaviour of both types of oligomers (Fig. 5). The effect was particularly relevant for A+ oligomers in GM1-enriched cells, where the median D value decreased by over one order of magnitude with respect to basal conditions.

4. Discussion

Gangliosides, in particular GM1, have been known for a long time to be involved in neurodegenerative conditions such as Alzheimer's disease [24,25]. Knowledge gained in the last ten years has clearly depicted raft GM1 as a main nucleator [14,26–28], interactor and concentrator of amyloid assemblies, particularly Aβ oligomers [29], which triggers the early event of amyloid cytotoxicity [30]. In particular, it has been reported that membranes may initiate AD through the formation of toxic Aβ amyloid fibrils on clustered, not diffused, GM1, which differed from those grown in solution [31]. These data highlight the importance of assessing GM1 mobility on the cell membrane to better define oligomer-membrane interaction and amyloid aggregate cytotoxicity.

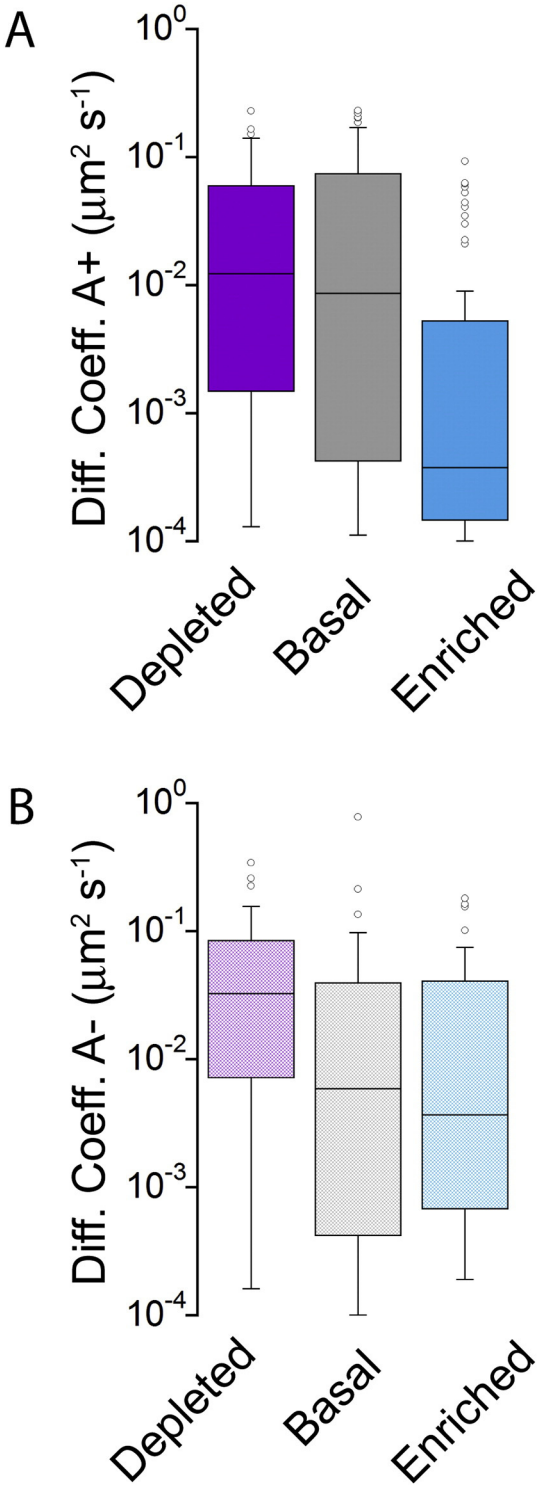

Fig. 5. The GM1 content influences the lateral diffusion of A+ and A− oligomers. A) and B) Box plot of diffusion coefficients of single A+ (n > 90 for each condition) and A− oligomers (n > 40 for each condition), respectively, in cells with basal GM1 content (grey) and in cells treated with 25 μM PDMP (purple) or with 100 μg/ml bovine brain GM1 (cyan). The oligomers were labelled with primary and secondary bFab antibodies coupled to s655QDs. ANOVA analysis of log normal distributed data, A+, F statistic = 15.3, $p < 0.0001$; A−, F statistic = 5.7, $p = 0.0046$.

In addition, Yanagisawa et al. identified a specific form of Aβ bound to GM1 in brains displaying the early pathological changes associated with AD suggesting that GM1-bound Aβ could act as a seed for aggregate growth [32]. These studies have contributed to focus the involvement of GM1 in the early events of Aβ aggregation and plaque

formation in AD. They were also supported by previous data showing that an increase in GM1 [33] together with altered distribution of GM1 and GM2 [25,34] are found in the brains of AD people in respect to healthy subjects; moreover, GM1 levels were found to be significantly increased in amyloid-positive synaptosomes obtained from AD brains [35], implying a pathological significance of GM1 increase at presynaptic neuritic terminals in AD. Therefore, the pivotal role of the aggregate-GM1 complexes can be true even in the case where raft associated proteins such as PrP have been shown to be affected by such interaction, which favours the assembly of membrane complexes triggering specific signalling cascades [36,37]. This further confirms the importance of studying the biophysical features of the Aβ-GM1 interaction and the effects of the latter on GM1 dynamics in the cell membrane.

Our recent research has shown that membrane lipid content, particularly where cholesterol and GM1 are concerned, modulates oligomer affinity to the membrane itself and hence their ability to affect membrane lipid order and permeability [13]. This holds true also for non-toxic variants of amyloid oligomers, whose different biophysical and structural properties result in different affinities to the cell membrane that, in turn, are modulated by membrane lipid content [11]. This has led us to propose that amyloid oligomer toxicity is not a property strictly inherent in oligomers but, rather a behaviour that emerges from a complex interplay between the structural and biophysical properties of both the membrane and the oligomers taken as a whole [38]. These data further highlight the importance of membrane GM1 and its clusters as a key modulator of amyloid cytotoxicity and foster further research to better elucidate from a biochemical, biological and biophysical perspective the relationship between oligomers and the cell membrane.

Here we used single molecule tracking experiments to investigate the effect on oligomer mobility of the interaction with GM1 on the plasma membrane of neuronal cells of two types of amyloid oligomers of the Aβ1–42 peptide grown at different times (A+ and A−), whose biophysical and cytotoxicity properties have been previously described [8]. In general, the single molecule approach represents a novel and valuable tool for investigating the biology of Aβ oligomers [39,40]. In our study, we investigated the type and extent of the mobility of either oligomer and of GM1 in cultured SH-SY5Y neuroblastoma cells. To do this, we employed a biophysical approach using both GM1 and oligomers labelled with quantum dot particles that enabled us to monitor the trajectories of either component and their lateral diffusion on the cell membrane. By using a similar approach, we have recently shown that distinct Aβ1–42 oligomers recognized by the conformation specific antibody OC and I11, respectively, diffuse differently on the plasma membrane of living cells on the basis of their structural properties [16] and that the same oligomers alter the mobility of single GM1 molecules upon binding [12]. Our data indicate that GM1 mobility on the cell is strongly affected by the interaction with the toxic A+ oligomers whereas A− oligomers do not interact. However, increasing GM1 content in the cell membrane matched a considerable reduction of oligomer mobility possibly resulting from GM1 clustering. The increase in GM1 content might affect the clustering and enlargement of existing raft platforms, or induce the formation of new ones. Alternatively, GM1 depletion by cell treatment with PDMP resulted in a significant increase of GM1 mobility possibly by decreasing platform size or by reducing platform stability. Since PDMP is a broad spectrum ganglioside-depleting agent, several different gangliosides, apart from GM1, may account, at least in part, for the observed increase in GM1 mobility in our experimental conditions. Such consideration agrees with previous data on the ability of some gangliosides, such as GM3, to bind Aβ1–42 oligomers [41–44], supporting a minor mechanistic role of other glycosphingolipids in addition to GM1 in mediating the increase of lateral diffusion of A+ oligomers on neuronal membranes. However the pivotal role of GM1 is supported by its abundance in neural tissue and by the data showing that its content gradually increases with age with parallel decrease of GM3 [45]; moreover, GM1 is increased in the CSF of AD patients [29]. It has also been found that the glycolipid-binding domain of Aβ does not recognize GM3 but GM1; the molecular determinants of the high affinity of such interaction have been reported [46]. Finally, the Selkoe group failed to detect an enrichment of brain lipids other than GM1 bound to Aβ in their recent paper supporting their evidence that Aβ oligomers preferentially bind to GM1 [29].

A large wealth of data has convincingly reported the involvement of membrane GM1 in AD pathogenesis through the promotion of Aβ binding and misfolding, the nucleation of its toxic aggregates, the recruitment of pre-formed oligomers, as well as the importance of lipid clusterization in all these events. Accordingly, the use of new biophysical techniques and approaches to study those events at the cell membrane level can provide useful information to better define the structural, biophysical and molecular modifications underlying the first steps of Aβ aggregation into cytotoxic assemblies as well as the ensuing early biochemical modifications of the involved cells.

Supplementary data to this article can be found online at http://dx.doi.org/10.1016/j.bbamem.2015.12.009.

Transparency document

The Transparency document associated with this article can be found in the online version.

Aknowledgements

We thank the Italian Ministry for Education, University and Research in the framework of the Flagship Project NANOMAX, the European Community's Seventh Framework Programme [FP7 2007–2013, LASERLABEUROPE GA 284464] and the Fondazione Cassa di Risparmio di Pistoia e Pescia [project no. 2014.0251].

References

[1] K.L. Viola, W.L. Klein, Amyloid beta oligomers in Alzheimer's disease pathogenesis, treatment, and diagnosis, Acta Neuropathol. 129 (2015) 183–206.
[2] W.F. Goure, G.A. Krafft, J. Jerecic, F. Hefti, Targeting the proper amyloid-beta neuronal toxins: a path forward for Alzheimer's disease immunotherapeutics, Alzheimers Res. Ther. 6 (2014) 42.
[3] K. Murakami, Conformation-specific antibodies to target amyloid beta oligomers and their application to immunotherapy for Alzheimer's disease, Biosci. Biotechnol. Biochem. 78 (2014) 1293–1305.
[4] I. Benilova, E. Karran, B. De Strooper, The toxic Abeta oligomer and Alzheimer's disease: an emperor in need of clothes, Nat. Neurosci. 15 (2012) 349–357.
[5] E.Y. Hayden, D.B. Teplow, Amyloid beta-protein oligomers and Alzheimer's disease, Alzheimers Res. Ther. 5 (2013) 60.
[6] R. Kayed, C.A. Lasagna-Reeves, Molecular mechanisms of amyloid oligomers toxicity, J. Alzheimers Dis. 33 (2013) S67–S78.
[7] M. Stefani, Structural polymorphism of amyloid oligomers and fibrils underlies different fibrillization pathways: immunogenicity and cytotoxicity, Curr. Protein Pept. Sci. 11 (2010) 343–354.
[8] A.R. Ladiwala, J. Litt, R.S. Kane, D.S. Aucoin, S.O. Smith, S. Ranjan, J. Davis, W.E. Van Nostrand, P.M. Tessier, Conformational differences between two amyloid beta oligomers of similar size and dissimilar toxicity, J. Biol. Chem. 287 (2012) 24765–24773.
[9] R. Kayed, E. Head, F. Sarsoza, T. Saing, C.W. Cotman, M. Necula, L. Margol, J. Wu, L. Breydo, J.L. Thompson, S. Rasool, T. Gurlo, P. Butler, C.G. Glabe, Fibril specific, conformation dependent antibodies recognize a generic epitope common to amyloid fibrils and fibrillar oligomers that is absent in prefibrillar oligomers, Mol. Neurodegener. 2 (2007) 18.
[10] M. Sakono, T. Zako, Amyloid oligomers: formation and toxicity of Abeta oligomers, FEBS J. 277 (2010) 1348–1358.
[11] E. Evangelisti, D. Wright, M. Zampagni, R. Cascella, C. Fiorillo, S. Bagnoli, A. Relini, D. Nichino, T. Scartabelli, B. Nacmias, S. Sorbi, C. Cecchi, Lipid rafts mediate amyloid-induced calcium dyshomeostasis and oxidative stress in Alzheimer's disease, Curr. Alzheimer Res. 10 (2013) 143–153.
[12] M. Calamai, F.S. Pavone, Partitioning and confinement of GM1 ganglioside induced by amyloid aggregates, FEBS Lett. 587 (2013) 1385–1391.
[13] E. Evangelisti, C. Cecchi, R. Cascella, C. Sgromo, M. Becatti, C.M. Dobson, F. Chiti, M. Stefani, Membrane lipid composition and its physicochemical properties define cell vulnerability to aberrant protein oligomers, J. Cell Sci. 125 (2012) 2416–2427.
[14] K. Sasahara, K. Morigaki, Y. Mori, Uptake of raft components into amyloid beta-peptide aggregates and membrane damage, Anal. Biochem. 481 (2015) 18–26.
[15] P.N. Lacor, M.C. Buniel, P.W. Furlow, A.S. Clemente, P.T. Velasco, M. Wood, K.L. Viola, W.L. Klein, Abeta oligomer-induced aberrations in synapse composition, shape, and density provide a molecular basis for loss of connectivity in Alzheimer's disease, J. Neurosci. 27 (2007) 796–807.

[16] M. Calamai, F.S. Pavone, Single molecule tracking analysis reveals that the surface mobility of amyloid oligomers is driven by their conformational structure, J. Am. Chem. Soc. 133 (2011) 12001–12008.
[17] S. Bonneau, M. Dahan, L.D. Cohen, Single quantum dot tracking based on perceptual grouping using minimal paths in a spatiotemporal volume, IEEE Trans. Image Process. 14 (2005) 1384–1395.
[18] H. Bannai, S. Lévi, C. Schweizer, M. Dahan, A. Triller, Imaging the lateral diffusion of membrane molecules with quantum dots, Nat. Protoc. 1 (2006) 2628–2634.
[19] M.V. Ehrensperger, C. Hanus, C. Vannier, A. Triller, M. Dahan, Multiple association states between glycine receptors and gephyrin identified by SPT analysis, Biophys. J. 92 (2007) 3706–3718.
[20] M.J. Saxton, K. Jacobson, Single-particle tracking: applications to membrane dynamics, Annu. Rev. Biophys. Biomol. Struct. 26 (1997) 373–399.
[21] M. Zampagni, D. Wright, R. Cascella, G. D'Adamio, F. Casamenti, E. Evangelisti, F. Cardona, A. Goti, B. Nacmias, S. Sorbi, G. Liguri, C. Cecchi, Novel S-acyl glutathione derivatives prevent amyloid oxidative stress and cholinergic dysfunction in Alzheimer disease models, Free Radic. Biol. Med. 52 (2012) 1362–1371.
[22] M. Bucciantini, D. Nosi, M. Forzan, E. Russo, M. Calamai, L. Pieri, L. Formigli, F. Quercioli, S. Soria, F. Pavone, J. Savistchenko, R. Melki, M. Stefani, Toxic effects of amyloid fibrils on cell membranes: the importance of ganglioside GM1, FASEB J. 26 (2012) 818–831.
[23] K. Palmano, A. Rowan, R. Guillermo, J. Guan, P. McJarrow, The role of gangliosides in neurodevelopment, Nutrients 7 (2015) 3891–3913.
[24] C.G. Gottfries, I. Karlsson, L. Svennerholm, Membrane components separate early-onset Alzheimer's disease from senile dementia of the Alzheimer type, Int. Psychogeriatr. 8 (1996) 365–372.
[25] M. Molander-Melin, K. Blennow, N. Bogdanovic, B. Dellheden, J.E. Månsson, P. Fredman, Structural membrane alterations in Alzheimer brains found to be associated with regional disease development; increased density of gangliosides GM1 and GM2 and loss of cholesterol in detergent-resistant membrane domains, J. Neurochem. 92 (2005) 171–182.
[26] K. Yanagisawa, GM1 ganglioside and Alzheimer's disease, Glycoconj. J. 32 (2015) 87–91.
[27] H. Ueno, T. Yamaguchi, S. Fukunaga, Y. Okada, Y. Yano, M. Hoshino, K. Matsuzaki, Comparison between the aggregation of human and rodent amyloid beta-proteins in GM1 ganglioside clusters, Biochemistry 53 (2014) 7523–7530.
[28] S. Sato, Y. Yoshimasa, D. Fujita, M. Yagi-Utsumi, T. Yamaguchi, K. Kato, M. Fujita, Self-assembled spherical complex displaying a gangliosidic glycan cluster capable of interacting with amyloidogenic proteins, Angew. Chem. Int. Ed. Engl. 54 (2015) 8435–8439.
[29] S. Hong, B.L. Ostaszewski, T. Yang, T.T. O'Malley, M. Jin, K. Yanagisawa, S. Li, T. Bartels, D. Selkoe, Soluble Abeta oligomers are rapidly sequestered from brain ISF in vivo and bind GM1 ganglioside on cellular membranes, Neuron 82 (2014) 308–319.
[30] M.A. Kostylev, A.C. Kaufman, H.B. Nygaard, P. Patel, L.T. Haas, E.C. Gunther, A. Vortmeyer, S.M. Strittmatter, Prion-protein-interacting Amyloid-beta oligomers of high molecular weight are tightly correlated with memory impairment in multiple Alzheimer mouse models, J. Biol. Chem. 290 (2015) 17415–17438.
[31] K. Matsuzaki, How do membranes initiate Alzheimer's disease? Formation of toxic amyloid fibrils by the amyloid β-protein on ganglioside clusters, Acc. Chem. Res. 47 (2014) 2397–2404.
[32] K. Yanagisawa, A. Odaka, N. Suzuki, Y. Ihara, GM1 ganglioside-bound amyloid beta-protein (A beta): a possible form of preamyloid in Alzheimer's disease, Nat. Med. 1 (1995) 1062–1066.
[33] K. Blennow, P. Davidsson, A. Wallin, P. Fredman, C.G. Gottfries, I. Karlsson, J.E. Månsson, L. Svennerholm, Gangliosides in cerebrospinal fluid in 'probable Alzheimer's disease', Arch. Neurol. 48 (1991) 1032–1035.
[34] Z. Pernber, K. Blennow, N. Bogdanovic, J.E. Månsson, M. Blomqvist, Altered distribution of the gangliosides GM1 and GM2 in Alzheimer's disease, Dement. Geriatr. Cogn. Disord. 33 (2012) 174–188.
[35] N. Yamamoto, T. Matsubara, T. Sato, K. Yanagisawa, Age-dependent high-density clustering of GM1 ganglioside at presynaptic neuritic terminals promotes amyloid beta-protein fibrillogenesis, Biochim. Biophys. Acta 1778 (2008) 2717–2726.
[36] J.W. Um, A.C. Kaufman, M. Kostylev, J.K. Heiss, M. Stagi, H. Takahashi, M.E. Kerrisk, A. Vortmeyer, T. Wisniewski, A.J. Koleske, E.C. Gunther, H.B. Nygaard, S.M. Strittmatter, Metabotropic glutamate receptor 5 is a coreceptor for Alzheimer Abeta oligomer bound to cellular prion protein, Neuron 79 (2013) 887–902.
[37] J.W. Um, H.B. Nygaard, J.K. Heiss, M.A. Kostylev, M. Stagi, A. Vortmeyer, T. Wisniewski, E.C. Gunther, S.M. Strittmatter, Alzheimer amyloid-beta oligomer bound to postsynaptic prion protein activates Fyn to impair neurons, Nat. Neurosci. 15 (2012) 1227–1235.
[38] C. Cecchi, M. Stefani, The amyloid-cell membrane system. The interplay between the biophysical features of oligomers/fibrils and cell membrane defines amyloid toxicity, Biophys. Chem. 182 (2013) 30–43.
[39] M. Renner, P.N. Lacor, P.T. Velasco, J. Xu, A. Contractor, W.L. Klein, A. Triller, Deleterious effects of amyloid beta oligomers acting as an extracellular scaffold for mGluR5, Neuron 66 (2010) 739–754.
[40] R.D. Johnson, D.G. Steel, A. Gafni, Structural evolution and membrane interactions of Alzheimer's amyloid-beta peptide oligomers: new knowledge from single-molecule fluorescence studies, Protein Sci. 23 (2014) 869–883.
[41] T. Ariga, K. Kobayashi, A. Hasegawa, M. Kiso, H. Ishida, T. Miyatake, Characterization of high-affinity binding between gangliosides and amyloid b-protein, Arch. Biochem. Biophys. 388 (2001) 225–230.
[42] M.O.W. Grimm, E.G. Zinser, S. Grösgen, B. Hundsdörfer, T.L. Rothhaar, V.K. Burg, L. Kaestner, T.A. Bayer, P. Lipp, U. Müller, H.S. Grimm, T. Hartmann, Amyloid precursor protein (APP) mediated regulation of ganglioside homeostasis linking Alzheimer's disease pathology with ganglioside metabolism, PLoS One 7 (2012), e34095.
[43] N. Yahi, A. Aulas, J. Fantini, How cholesterol constrains glycolipid conformation for optimal recognition of Alzheimer's b amyloid peptide (Abeta1-40), PLoS One 5 (2010), e9079.
[44] N. Yamamoto, Y. Hirabayashi, M. Amari, H. Yamaguchi, G. Romanov, W.E. Van Nostrand, K. Yanagisawa, Assembly of hereditary amyloid b-protein variants in the presence of favorable gangliosides, FEBS Lett. 579 (2005) 2185–2190.
[45] L. Svennerholm, K. Boström, B. Jungbjer, L. Olsson, Membrane lipids of adult human brain: lipid composition of frontal and temporal lobe in subjects of age 20 to 100 years, J. Neurochem. 63 (1994) 1802–1811.
[46] N. Yahi, J. Fantini, Deciphering the glycolipid code of Alzheimer's and Parkinson's amyloid proteins allowed the creation of a universal ganglioside-binding peptide, PLoS One 9 (2014), e104751.